Egyptian Journal of Chemistry

http://ejchem.journals.ekb.eg/

Synthesis, Corrosion inhibition study and DFT calculation of two New Azo Compounds

[1]Dhaif, Hawraa K[*]; [2]Jasim, Ekhlas Q; [1]Rafid. H. Al-Asadi and [1]Mohammed K M;

Department of Chemistry, College of Education for pure sciences, University of Basrah, 61004 Basrah, Iraq

Abstract

New derivatives of heterocyclic azo compounds were synthesized by free catalyst reaction. The structure of the synthesized compound was confirmed by various techniques such as ^{1}H-NMR, ^{13}C-NMR, and mass spectrometry. The synthesized derivatives have been studied and evaluated as corrosion inhibition for carbon steel in 0.1 M HCl solution. The prepared derivatives 1,1'-(((1E,1'E)-(5-nitro-1,3-phenylene)bis(diazene-2,1-diyl))bis(4-methyl-3,1-phenylene))bis(1H-pyrrole-2,5-dione) (NAH) and 1,1'-(((1E,1'E)-(5-nitro-1,3-phenylene)bis(diazene-2,1-diyl))bis(3-hydroxy-4,1-phenylene))bis(1H-pyrrole-2,5-dione) (NAM) showed 89.22% and 91.30% inhibition efficiencies at a concentration of 1 x 10-3 M, respectively. It is found that the adsorption isotherm of these derivatives conforms to the Langmuir model. In addition, density functional theory is used to theoretically estimate HOMO, LUMO, and other chemical quantum parameters. The results indicate that the synthesized derivative exhibits corrosion inhibitory properties, and derivative NAM is more effective than derivative NAH. In addition, the theoretical results are consistent with experimental data.

Keywords: Azo compounds, N-(4-hydroxylpheneyl)maleimide, Tafel curve, Corrosion inhibition, DFT

1. Introduction

Corrosion is considered to be the main problem that limits the widespread use of metal materials. Corrosion-related damage can lead to increased maintenance costs. Therefore, it is more necessary to protect the materials used [1,2]. Many researchers try to develop methods to reduce metal corrosion. Metal materials react with their surrounding media based on the electrochemical corrosion process. Various environmental conditions, such as acidity, salinity, moisture and aeration, are all causes of corrosion of iron or iron alloy materials. Corrosion can deteriorate material properties, such as chemical, physical and mechanical properties[3,4].

One way to achieve this goal involves the use of organic inhibitors that can effectively reduce or prevent the corrosive effects of metals and metal alloys. Organic compounds can form a protective layer to reduce or prevent many corrosive factors from penetrating the metal surface. Therefore, the success of this method reduces the formation of metal surface defects. Organic inhibitors used to prevent

corrosion of steel surfaces include organic compounds containing sulfur, nitrogen, and/or oxygen atoms [5,6].

Azo compounds are an important class of organic compounds that can be used to synthesize organic compounds[7,8]. Azo compounds can be used in a variety of applications, such as textiles, leather, cosmetics, pharmaceutical reagents, and even corrosion inhibitors[9,10], for example as corrosion inhibitors for carbon steel [4-9] and mild steel [12,13], and aluminum [14,15]. The protection method involves the chemical reaction between the azo group and various substituted aromatic bonds present on the metal surface. This process displays a strong color for the compound in the entire visible light range. In addition, these chemical reactions also enhance the stability of metals, require lower production costs, and use simple synthetic processes [16,17].

We have synthesized new maleimide derivatives and tested their efficiency on carbon steel materials in this work. These derivatives were dissolved in 0.1 M HCl

and tested using potentiodynamic polarization techniques to evaluate their corrosion inhibition efficiency. In addition, computer simulations were performed to calculate some quantum chemical parameter values to study the relationship between theory and actual performance.

2. Experimental method

Chemicals and solvents were purchased from Sigma-Aldrich (USA). Use pre-coated silica gel 60, UV 254 TLC plates to monitor the progress of the reaction using thin-layer chromatography (TLC) for all synthetic compounds. 1HNMR and 13CNMR spectra were recorded on Bruker Inovo AV-400 spectrometer (Iran), using DMSO-d6 as the solvent. The proton of the decoupling value (J) is expressed in Hz, and the melting point of the compound is measured with the help of a capillary tube using a Gallenkamp melting point apparatus. The precise mass spectra of the synthesized compounds were run on JEOL JMS-5X 10217 of EI type (Iran).

2.1. Synthesis

Synthesis of 1,1'-(((1E,1'E)-(5-nitro-1,3-phenylene)bis(diazene-2,1-diyl))bis(4-methyl-3,1-phenylene))bis(1H-pyrrole-2,5-dione) NAH

The cooled solution of 5-nitrobenzene-1,3-diamine (0.01 mole) dissolved in a dilute hydrochloric acid solution (concentrated hydrochloric acid: H_2O, 1:1 v/v) is kept in an ice bath (≤ 5 °C). $NaNO_2$ (0.02 mole) dissolved in water (10 mL) was added dropwise to the above solution. The mixture was continuously stirred under an ice bath. According to reference[7,8], N-(4-methylphenyl)maleimide) (0.02 mole) was added to the above content. Dissolve the resulting mixture in NaOH solution (10% wt/v, 20 mL) at 5°C. The resulting mixture was cooled in an ice bath and stirred for another 20 minutes. The resulting precipitate was then filtered and recrystallized from glacial acetic acid and washed with methanol to remove traces of glacial acetic acid. Finally, the precipitate formed is filtered, washed with distilled water, and the desired product is dried in an oven at 50°C for 24 hours.

Red-brown solid, yield 55%, m.p 161–163 °C. ^{1}H-NMR (500 MHz, DMSO-d$_6$) δ (ppm): 2.22, s (6H, CH$_3$), 6.32, d (2H, J = 10 MHz, CH=CH), 6.47, d (2H, J = 10 MHz, CH=CH), 7.14–7.65, m (9H,

Ar–H). ^{13}C-NMR (125 MHz) δ (ppm): 16.70, 112.51, 117.76, 119.92, 122.57, 127.43, 129.36, 129.52,131.97, 135.91, 138.51, 144.79, .171.71, MS [EI]$^+$ m/z 549[M]$^+$.

Synthesis of 1,1'-(((1E,1'E)-(5-nitro-1,3-phenylene)bis(diazene-2,1-diyl))bis(3-hydroxy-4,1-phenylene))bis(1H-pyrrole-2,5-dione) NAM

The cooled solution of 5-nitrobenzene-1,3-diamine (0.01 mole) dissolved in a dilute hydrochloric acid solution (concentrated hydrochloric acid: H_2O, 1:1 v/v) is kept in an ice bath (≤ 5 °C). $NaNO_2$ (0.02 mole) dissolved in water (10 mL) was added dropwise to the above solution. The mixture was continuously stirred under an ice bath. According to reference [7,8], N-(4-methylphenyl)maleimide) (0.02 mole) was added to the above content. Dissolve the resulting mixture in NaOH solution (10% wt/v, 20 mL) at 5°C. The resulting mixture was cooled in an ice bath and stirred for another 20 minutes. The resulting precipitate was then filtered and recrystallized from glacial acetic acid and washed with methanol to remove traces of glacial acetic acid. Finally, the precipitate formed is filtered, washed with distilled water, and the desired product is dried in an oven at 50°C for 24 hours.

Light brown powder; yield 67%, m.p. 178-180 °C, ^{1}H-NMR (DMSO, 500 MHz) δ: 2.83, s (2H, OH) , 6.285, d (2H, J= 10 MHz, CH=CH), 6.47, d (2H, J= 10 MHz, CH=CH), 6.97-7.10, m (9H, Ar–H). ^{13}C-NMR (125 MHz) δ (ppm): 112.52, 117.75, 119.92, 122.55, 126.46, 128.33, 129.82,131.93, 135.81, 138.5**5**, 143.99, .171.63, MS [EI$^+$] m/z (%): 553[M]$^+$.
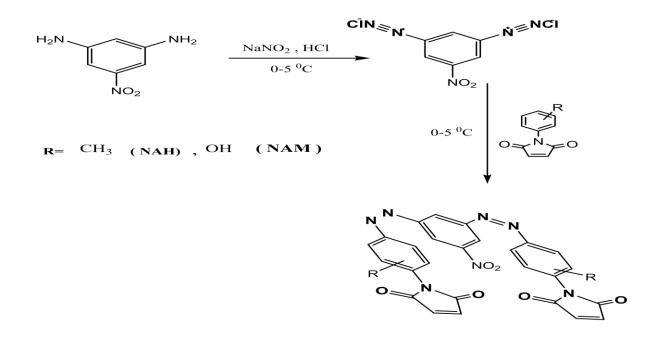
3. Results and Discussion
3.1. Synthesis and characterization
In this study, the researchers diazotized Benzene-1,4-diamine and 4,4'-oxydianiline in the presence of chemical catalysts like dilute HCL acid and sodium nitrite, to yield a diazonium salt. These compounds were coupled with N-(4-Methylphenyl)maleimide for synthesizing the Azo compounds NAH and NAM, using Scheme 1.

They confirmed the structure of these Compounds NAH and NAM with the help of ^{1}H-NMR, ^{13}C-NMR, and mass spectroscopy. The ^{1}H-NMR spectra showed that the protons present in the alkene group (HC=CH) of these compounds could be detected as two doublet signals at 6.285-6.32 and 6.47 ppm. A singlet signal was noted at 2.22 ppm for CH_3 and 2.83 ppm for OH in Compounds NAH and NAM, which was attributed to the protons present in the methyl group in these compounds. Furthermore, the protons existing in the aromatic groups showed their presence in the form of multiple signals between
.

7.14–7.65 ppm and 6.97–7.10 ppm for Compounds NAH and NAM, respectively.

On the other hand, the ^{13}C-NMR spectra displayed the following signals, which characterized the structure of the molecules: 171.71 and 171.63 ppm (C=O); 135.91 and 135.81 ppm (HC=CH, alkenes) ; 112.51-131.97 ppm (C=C, aromatics), 16.70 ppm (CH_3). Finally, the mass spectra of Compounds NAH and NAM indicated the presence of a molecular ion peak in the form of a base peak at m/z 549 and 553, respectively.

Scheme 1. Chemical structure of the synthesized compounds

3.2. Potentiodynamic Polarization Curves

To establish the mechanism and the kinetic in the anodic and cathodic reactions, the efficiency of the synthesis organic compounds (NAH, NAM) as a corrosion inhibitor was evaluated on N110 mild steel in 0.1M HCl at room temperature via potentiodynamic polarization curves. The Figure 1 shows the polarization

$$\theta = \left[1 - \frac{Icorr(inh)}{Icorr}\right]$$

Where I_{corr} and I_{corr} (inh) are the corrosion current in the absence and in the presence of inhibitor, respectively.

As the inhibitor concentration increased, the current density decreased proportionally, suggesting that

inhibitor molecules were absorbed into the metal surface, preventing the aggressive species from accessing the metal surface from the corrosive media [32, 33]. This phenomenon allows the corrosion rate to decrease in the presence of increased inhibitor and inhibitor efficiency, confirming that oxidation-reduction reactions have been influenced by the maximum efficiency of the block of the active sites of 94.03 percent when the inhibitor is present in $1 \times 10^{-3} M$.

3.3. Effect of Temperature

With the aid of Tafel Plots, the researchers investigated the effect of temperature (25-45 °C) on mild steel/acid after being submerged (180 minutes) in varying concentrations of Inhibitor Compounds

NAH and NAM. When the temperature was reduced, the findings illustrated a difference in the IE of the two compounds. On the other hand, the existence of a possible physisorption mechanism was demonstrated by an increase in temperature, which was substantially improved with increasing temperature. [17] The effects of this effect are presented in Table 5, while Fig. 2 shows the variance noted as a function of temperature at the concentration of 1×10^{-3}M in the IE (percent).

They calculated the activation energy, Ea, for the corrosion process as follows:

$$\ln\left(\frac{r2}{r1}\right) = (Ea(\frac{T1}{T2}))/R(T2*T1)$$

Where:

r_1= corrosion rate at a temperature of 308 K; r_2= corrosion rate at a temperature of 318 K; Ea= activation energy; R= gas constant (8.3143 J.K^{-1}.mol^{-1}); while T_1 and T_2= Absolute temperatures (K)

Table 1: Activation energy for dissolution of mild - steel in 0.1 M HCl in the different of (10^{-3}) concentration.

Comp.	Conc. [M]	Activation Energy KJ mol^{-1}
HCl	0.00	1.503
NAH	1×10^{-3}	6.625
NAM	1×10^{-3}	36.640

In addition, the decrease in the IE values noted when the temperature increased suggested a process of physisorption adsorption [19,20]. Based on the findings, the researchers concluded that with the help of the physisorption principle, the inhibitor compounds adsorbed effectively on the surface of the mild steel.

They calculated the Free energy of adsorption (ΔG) using the formula below[18].

$$\Delta G = RTln[55.5\theta lC(1-\theta)]$$

Where:

θ= degree of coverage on the metal surface, C= concentration of inhibitors (1×10^{-4}M), R= gas constant (8.3143J.K^{-1}.mol^{-1}), T= Absolute temperature (K)

And For calculating the entropy ΔS and enthalpy ΔH apply the alternative formulation of the Arrhenius equation is the transition state equation[19].

$$Rcorr = \frac{RT}{Nh}\exp\left[\frac{\Delta S}{R}\right]\exp\left[-\frac{\Delta H}{RT}\right]$$

Where:

R_{corr} = corrosion rate, R= gas constant (8.3143J.K^{-1}.mol^{-1}), T= temperature (K), N=Avogadro 's number (6.2×10^{-23}), h= plank 's constant (6.62×10^{-34} J.S)

The findings showed that the activation energy was 2.354, 6.239 and 11.358, respectively, for HCl, Compounds I and II. The researchers concluded that the positive ΔH values suggested that the adsorption

of the inhibitor compounds on the surface of the mild steel was an endothermic operation, based on the results presented in Table 4. In the absence/presence of inhibitor compounds, on the other hand, the ΔS values were seen to be negative. The activation complex was thus characterized as a rate-defining phase indicating the association instead of the disassociation, indicating that when the reactants formed an activated complex, the disorder decreased [22].

In addition, the negative ΔG values showed that the Azo Corrosion Inhibitory Compounds (I and II) were adsorbed spontaneously on the surface of the metal compounds. These findings also suggested that the inhibitor compounds could interact with mild-steel surfaces very effectively [23].

It was noted that when the temperatures were elevated, the ΔG displayed a negative rise. This phenomenon suggested that when the temperature was elevated, the adsorption was very favorable and the desorption of inhibitors from mild steel surfaces was dominant [24].

3.4. Adsorption Isotherm

Adsorption isotherms help in understanding the inhibition mechanism involved in a corrosion chemical reaction. The common adsorption isotherms are seen to be Freundlich, Frumkin, Langmuir and Temkin isotherm. In this study, the data showed the best fit with the Langmuir isotherm. When the researchers plotted (C/θ) *vs* inhibitor concentration

(C), a straight line was noted as described in Fig. 4. The results also indicated that the inhibitor compounds, NAH and NAM could adsorb onto the mild steel metal surfaces based on the Langmuir isotherm model as follows[20]:

$$C/\theta = 1/K + C$$

Where:

K= is the equilibrium constant of the adsorption process.

Table 2: The Values of corrosion parameters for the corrosion of Mild-steel in 0.1M HCl by galvanostatic polarization in presence inhibitor NAH

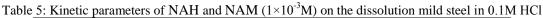| Conc (M)	CR (mpy)	Icorr (A)	Ecorr (V)	βc (A/V)	βa (A/V)	IE %	Θ
0.00	3.383	0.00233	-0.739	-2.884	5.951	–	–
1×10^{-5}	2.107	0.000266	-0.620	-5.051	5.855	88.56	0.8856
1×10^{-4}	1.338	0.000230	-0.617	-4.829	6.643	90.11	0.9011
1×10^{-3}	1.103	0.000139	-0.577	-5.574	6.011	94.03	0.9403

Table 3: The Values of corrosion parameters for the corrosion of mild-steel in 0.1M HCl by galvanostatic polarization in presence inhibitor NAM

Conc (M)	CR (mpy)	Icorr (A)	Ecorr (V)	βc (A/V)	βa (A/V)	IE %	Θ
0.00	3.383	0.00233	-0.739	-2.884	5.951	–	–
1×10^{-5}	1.312	0.000211	-0.687	-4.887	6.679	90.94	0.9094
1×10^{-4}	1.215	0.000197	-0.693	-5.003	6.874	91.54	0.9154
1×10^{-3}	1.117	0.000178	-0.604	-4.846	6.798	92.35	0.9235

Table 4: Effect of inhibitors NAH and NAM (1×10^{-3}M) on the dissolution mild steel in 0.1M HCl in the different temperature

Comp	Temp (°C)	CR (mpy)	Icorr (A)	Ecorr (V)	βc (A/V)	βa (A/V)	%IE	Θ
Blank	25	3.383	0.00233	-0.739	-2.884	5.951	-	-
	35	3.489	0.00240	-0.612	-4.961	6.594	-	-
	45	3.554	0.00245	-0.660	-6.263	6.472	-	-
NAH	25	1.103	0.000139	-0.577	-5.574	6.011	94.03	0.9403
	35	1.109	0.000166	-0.577	-5.162	6.545	93.04	0.9304
	45	1.203	0.000221	-0.593	-5.053	6.433	90.96	0.9096
NAM	25	1.117	0.000178	-0.604	-4.846	6.798	92.35	0.9235
	35	1.117	0.000238	-0.601	-4.977	6.575	90.08	0.9008
	45	2.103	0.000260	-0.590	-4.833	5.454	89.38	0.8938

Table 5: Kinetic parameters of NAH and NAM (1×10^{-3}M) on the dissolution mild steel in 0.1M HCl

Compounds	Tem.(K)	Activation parameters (KJmol-1)		
		ΔH	-ΔS	-ΔG
Blank		0.00062	0.1580	_
NAH	298	0.02229	0.1694	33.896
	308			34.614
	318			34.987
NAM	298	0.01081	0.1634	33.237
	308			33.624
	318			34.51

Fig. 1: Galvanostatic polarization curves of mild-steel in 0.1M HCl in the different concentrations of Inhibitors NAH(A) and NAM(B).

Fig. 2: Galvanostatic polarization curves of Mild-steel in 0.1M HCl at different   temperatures of inhibitor **NAH(A)**, c: presence of inhibitor **NAM(B)**.
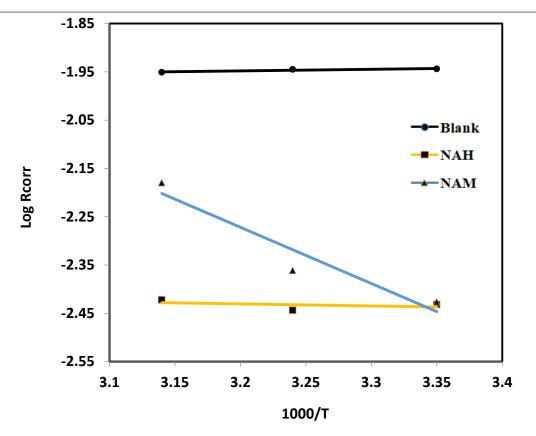
Fig 3: Arrhenius plots Log Rcorr ⁄T) *vs. 1⁄*T for mild-steel in different Additives of inhibitors NAH and NAM
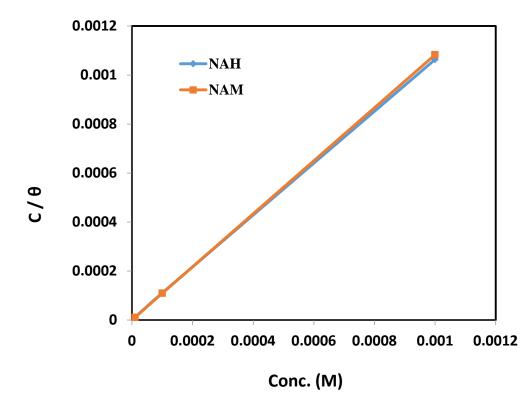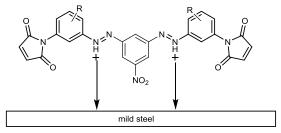

Fig 4: Langmuir Adsorption Isotherm Model for inhibitors in 0.1M HCl on the Surface of Conclusions
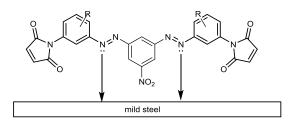
Mechanism of Inhibition

The azo compounds inhibit mild steel corrosion in 0.1 M HCl through adsorption at the mild-steel solution interface, according to the electrochemical results. Organic molecules can adsorb on metal surfaces in one of three ways, according to popular belief.
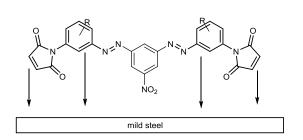
1. The charge of molecules interacts with the charge of the charged metal electrostatically.

2. Interaction of unshared electron pairs in the molecule with metal.

3. Pi-electrons interact with metal.

Theoretical study

The calculations for the **NAM** and **NAH** molecules were done using the Density Functional Theory (DFT) method using the Becke exchange plus Lee-Yang-Parr correlation (BLYP) theory level. The basis set used was a Double Numerical plus d-functions (DND). Material Stuio-DMol3 ver. 5.5 software was used to extract the output file. Molecular orbital energy values E_{LUMO} and E_{HOMO} were extracted from the file, and calculated some quantum chemical parameters by using the equations mentioned below [21,22].

Ionization potential	$IP = -E_{HOMO}$
Electrone affinity	$EA = -E_{LUMO}$
Electronegativity	$\chi = -1/2\,(E_{HOMO} + E_{LUMO})$
Chemical hardness	$\eta = -1/2\,(E_{HOMO} - E_{LUMO})$
Global electrophilicity	$\omega = \chi^2/2\eta$
Absolute softness	$\sigma = 1/\eta$
Number of electrones transferred	$\Delta N = \chi_{Fe} - \chi_{inh}\,/\,2(\eta_{Fe} + \eta_{inh})$

Results and discussion

Theoretical calculations

Chemical molecules' HOMO and LUMO orbitals, as well as their energy gaps, are crucial in determining their reactivity. The adsorption of the inhibitor on the metal surface can occur as a result of donor-acceptor interactions between the π-electrons of the heterocyclic compound and the unoccupied d-orbital of the metal surface atoms, according to a review of the literature. [23]. The capacity of inhibitor compounds to adsorb on a mild steel surface coupon is linked to HOMO and LUMO [20,24]. The ability of a molecule to donate electrons is referred to as HOMO, whilst the ability to take electrons is referred to as LUMO [25]. The high value of E_{HOMO}, as well as the low values of E_{LUMO} and $\Delta E_{LUMO-HOMO}$ is a significant indicator of excellent inhibition efficiency [26], due to the low energy required to remove electrons from an occupied orbital. Figure 5, shows the geometry optimization and electronic density of HOMO and LUMO orbitals' of studied molecules were observed the center of electronic donating sits on oxygen atoms, nitrogen, and phenyl rings.

When we compare the two molecules **NAM** and **NAH**, the calculations show that the **NAH** has the highest HOMO value and lowest LUMO and energy gap values, Table 1. This result is in good agreement with experimental observations. Ionization potential (IP) and absolute electronegativity (χ) are important descriptors of the chemical reactivity of atoms and molecules. High values of (IP) and (χ) designate high stability and chemical inertness while small values specify high reactivity of the atoms and molecules [27]. From values of ionization potential and absolute electronegativity in Table 1, we observed the molecule **NAH** has high inhibition efficiency.

Global hardness (η) and global softness (σ) are the main properties to measure the stability and reactivity of molecules. It is apparent that the chemical hardness fundamentally indicates the resistance towards the deformation or polarization of the electron cloud of the atoms, ions or molecules under small perturbation of chemical reaction. A hard molecule has a great energy gap and a soft molecule has a small energy gap [28]. Molecule **NAH** has shown more softness properties and less hardness properties, so it's expected to have more inhibition efficiency. Global electrophilicity (ω) serves as an important marker of reactivity and may be used to compare molecules on their electron-donating ability [29]. High global electrophilicity implies that the molecule behaves as an electrophile. In the study, molecule **NAH** is electrophilic, and it highest inhibition. These results correspond to what we have achieved in the practical study.

The calculated values of the Number of electrons transferred (ΔN) reveal that the electron donation-induced inhibition efficiency accords with Lukovit's findings. [30]. By boosting the electron-donating ability of these inhibitors to donate electrons to the metal surface, the inhibition efficiency rises if N < 3.6 is used. The results indicate that molecules **NAM**

and **NAH** have corrosion inhibition efficiencies. Thus, the highest fraction of electrons transferred (2.400) is associated with the best inhibitor **NAH**. This is in good agreement with the experimental observations.

The dipole moment (μ) was another quantum chemical parameter that was important for corrosion prevention efficacy. It is related to the electrons distribution and bond polarity [31]. The high value of (Debye) is likely to increase the adsorption of the chemical compound on the metal surface [32]. The energy of the deformability increases with the increase in μ, making the molecule easier to adsorb at the iron (Fe) surface [33], the dipole moment for **NAH** molecule is the highest (7.802Debye). As a result, the inhibition efficiency and the dipole moment have a direct relationship.

As a result, we note that molecule **NAH** has more inhibitory properties of iron corrosion than molecule **NAM**, this may be due to the difference in the chemical structure of the two molecules, where molecule **NAH** contains an effective OH group on the phenyl ring instead of the CH_3 group in molecule **NAM**, which may cause some steric hindrance to the action of the inhibitor.

Table 6: Quantum chemical parameters values of **NAM** and **NAH** molecules

Parameters	NAM	NAH
E_{HOMO} (eV)	-5.183	-4.909
E_{LUMO} (eV)	-3.592	-3.809
$\Delta E_{LUMO-HOMO}$ (eV)	1.591	1.100
μ (Debye)	5.611	7.802
IP(eV)	5.183	4.909
EA(eV)	3.592	3.809
χ (eV)	4.387	4.359
η (eV)	0.795	0.550

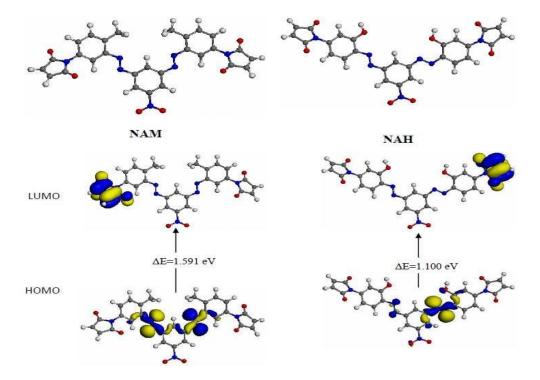|		
ω (eV)	12.099	17.273
σ (eV)	1.257	1.818
ΔN (eV)	1.642	2.400

Fig.5: Geometry optimization and HOMO, LUMO orbital's of **NAM** and **NAH** molecules

4. Conclusions

In this study, novel azo compounds were synthesized NAH and NAM which can be used as effective Corrosion inhibitors. These compounds were dissolved in 0.1M HCl solution and allowed to adsorb onto the mild steel surface at varying temperatures. The Inhibitory Efficiency (%) values indicated that the concentration of the synthesized compounds which get adsorbed on the metal surface is directly proportional to the temperature of adsorption. Thus, the inhibition due to corrosion of the azo dyes could be attributed to the adsorption onto the metal surfaces. These azo compounds are seen to be a mixed form of inhibitors and they tend to follow the Langmuir adsorption isotherm.

Based on the theoretical analysis of the synthesized compounds, the researchers stated that these compounds displayed corrosion inhibitory properties for the Fe alloys. Additionally, the IE of Compound NAM was higher than NAH This could be attributed to the presence of an oxo-diphenyl group in Compound NAM. Furthermore, the experimental and theoretical results showed a good agreement.

References

[1] K.C. Emregül, O. Atakol, "Corrosion inhibition of mild steel with Schiff base compounds in 1 M HCl", Materials chemistry and physics, 82 (2003), 188–193, https://doi.org/10.1016/S0254-0584(03)00204-9.

[2] H.H. Al-doori, M.S. Shihab, "Study of Some [N-substituted] p -aminoazobenzene as Corrosion

Inhibitors for Mild-Steel in 1M H$_2$SO$_4$", Al-Nahrain Journal of Science ,17 (2014), 59–68.

[3] H.K. Dhaef, E.Q. Jasim, Z.A. Muhajjar, A.A. Shanta, "Corrosion Inhibition of Mild-Steel in 0 . 5 M HCl using some prepared", Mediterranean Journal of Chemistry, 9 (2019), 290–304.

[4] M. Abdallah, B.H. Asghar, I. Zaafarany, A.S. Fouda, "The Inhibition of Carbon Steel Corrosion in Hydrochloric Acid Solution using Some Phenolic Compounds", Int. J. Electrochem. Sci, 7 (2012), 282–304.

[5] A.E. Jawad, M.S. Shihab, " Pyridine Derivatives as Corrosion Inhibitors for Mild Steel in 1M H$_2$SO$_4$ Solution", Journal of Iraqi Industrial Research", 4 (2017), 11–21.

[6] E.Q. Jasim, "Investigation of Salvadora persica Roots Extract as Corrosion Inhibitor for Mild Steel in 1 M HCl and in Cooling Water", Chemistry and Materals Research, 7 (2015), 147–159.

[7] M.K. Mohammed, F.A. Almashal, A.M. Jassem,"1,3-Dipolar Cycloaddition: Free Catalytic Synthesis and Esophageal Cancer Activity of New 1,2,3-Triazole-Oxydianiline-Maleimide Hybrids", Egyptian Journal of Chemistry, 64 (2021), 47–53. https://doi.org/10.21608/EJCHEM.2020.29188.2629.

[8] H.K. Dhaef, R.H. Al-Asadi, A.A. Shenta, M.K. Mohammed, "Novel Bis Maleimide Derivatives Containing Azo Group: Synthesis, Corrosion Inhibition, and Theoretical Study", Indones. J. Chem. 21 (2021) 1212. https://doi.org/10.22146/ijc.64614.

[9] A.S. Fouda, A.H. El-azaly, R.S. Awad, A.M. Ahmed, "New Benzonitrile Azo Dyes as Corrosion Inhibitors for Carbon Steel in Hydrochloric Acid Solutions", Int. J. Electrochem. Sci, 9 (2014), 1117–1131.

[10] M. Abdallah, M.M. Alfakeer, N.F. Hasan, A.M. Alharbi, E.M. Mabrouk, "Polarographic Performance of Some Azo Derivatives Derived from 2-amino-4-hydroxy Pyridine and Its Inhibitory Effect on C-steel Corrosion in Hydrochloric acid", Oriental Journal of Chemistry V 35, 1(2019), 98.

[11] M. Abdallah, A.S. Fouda, S.A. Shama, E.A. Afifi, "Azodyes as corrosion inhibitors for dissolution of C-steel in hydrochloric acid solution", African Journal of Pure and Applied Chemistry, 2(2008), 83–91.

[12] A.M. Nagiub, M.H. Mahross, H.F.Y. Khalil, B.N.A. Mahran, "Azo Dye Compounds as Corrosion Inhibitors for Dissolution of Mild Steel in Hydrochloric Acid Solution", Portugaliae Electrochimica Acta, 31(2013), 119–139. https://doi.org/10.4152/pea.201302119.

[13] A. Ismail, "A REVIEW OF GREEN CORROSION INHIBITOR FOR MILD STEEL IN SEAWATER", ARPN Journal of Engineering and Applied Sciences, 11(2016), 8710–8714.

[14] E.M. Mabrouk, H. Shokry, K.M.A.B.U. Al-naja, "Inhibition of aluminum corrosion in acid solution by mono- and bis-azo naphthylamine dyes", Chemistry of metals and alloys, Part 1, 4(2011), 98–106.

[15] I.A. Mohammed, A. Mohammed, "Synthesis of new azo compounds based on n-(4-hydroxypheneyl)maleimide and n-(4-methylpheneyl)maleimide", Molecules, 15(2010), 7498–7508. https://doi.org/10.3390/molecules15107498.

[16] E.M. Mabrouk, S. Eid, M.M. Attia, "Corrosion inhibition of carbon steel in acidic medium using azo chromotropic acid dye compound", Journal of Basic and Environmental Sciences, 4(2017), 351–355.

[17] A.S. Fouda, M. Gaber, M. Fakeeh, "Azo Compounds as Green Corrosion Inhibitor for Carbon Steel in Hydrochloric Acid Solution : Corrosion Inhibition and Thermodynamic Parameters", 12(2017), 8745–8760. https://doi.org/10.20964/2017.09.33.

[18] S.M.A. Hosseini, A. Azimi, I. Sheikhshoaei, M. Salari, "Corrosion inhibition of 302 stainless steel with schiff base compounds", J. Iran. Chem. Soc., 7(2010), 799–806.

[19] B. Idir, F. Kellou-Kerkouche, "Experimental and theoretical studies on corrosion inhibition performance of phenanthroline for cast iron in acid solution", J. Electrochem. Sci. Technol. 9(2018), 260–275.

[20] A. Yousefi, S. Javadian, J. Neshati, "A new approach to study the synergistic inhibition effect of cationic and anionic surfactants on the corrosion of mild steel in HCl solution", Ind. Eng. Chem. Res., 53(2014), 5475–5489.

[21] A. Zarrouk, B. Hammouti, H. Zarrok, R. Salghi, M. Bouachrine, F. Bentiss, S.S. Al-Deyab, "Theoretical study using DFT calculations on

inhibitory action of four pyridazines on corrosion of copper in nitric acid", Res. Chem. Intermed., 38(2012), 2327–2334.

[22] Y. Karzazi, M.E. Belghiti, F. El-Hajjaji, B. Hammouti, "Density functional theory modeling and monte carlo simulation assessment of N-substituted quinoxaline derivatives as mild steel corrosion inhibitors in acidic medium", J Mater Env. Sci., 7(2016), 3916–3929.

[23] A. Domenicano, I. Hargittai, I. Hargittai, others, Accurate molecular structures: their determination and importance, Oxford University Press, (1992).

[24] H.J. Habeeb, H.M. Luaibi, T.A. Abdullah, R.M. Dakhil, A.A.H. Kadhum, A.A. Al-Amiery, "Case study on thermal impact of novel corrosion inhibitor on mild steel", Case Stud. Therm. Eng., 12(2018), 64–68.

[25] M.E. Ikpi, F.E. Abeng, B.O. Okonkwo, "Experimental and computational study of levofloxacin as corrosion inhibitor for carbon steel in acidic media", World News Nat. Sci., 9(2017), 79–90.

[26] S. Hadisaputra, A.A. Purwoko, F. Wajdi, I. Sumarlan, S. Hamdiani, "Theoretical study of the substituent effect on corrosion inhibition performance of benzimidazole and its derivatives", Int. J. Corros. Scale Inhib., 8(2019), 673–688.

[27] C. Chemistry, S.G. Agalave, S.R. Maujan, V.S. Pore, Click Chemistry: 1,2,3-triazole as pharmacophore, (n.d.), 1–24.

[28] R. Hasanov, M. Sad\iko\uglu, S. Bilgiç, "Electrochemical and quantum chemical studies of some Schiff bases on the corrosion of steel in H_2SO_4 solution", Appl. Surf. Sci., 253(2007), 3913–3921.

[29] P.K. Chattaraj, Electrophilicity Index, Chem. Rev., 111(2011), PR43--PR75.

[30] I. Lukovits, E. Kalman, F. Zucchi, "Corrosion inhibitors—correlation between electronic structure and efficiency", Corrosion. 57(2001), 3–8.

[31] R.H. Al-asadi, Synthesis , "DFT Calculation and Biological Activity of Some Organotellurium Compounds Containing Azomethine Group", Elect. J. Chem, 11, 7(2019), 402.

[32] M. Filali, E.M. El Hadrami, A. Ben-Tama, B. Hafez, I. Abdel-Rahman, A. Harrach, H. Elmsellem, B. Hammouti, M. Mokhtari, S.E. Stiriba, others, "3, 6-Di (pyridin-2-yl) pyridazine derivatives as original and new corrosion inhibitors in support of mild steel: Experimental studies and DFT investigational", Int. J. Corros. Scale Inhib. 8 (2019) 93–109.

[33] N. Fu, S. Wang, Y. Zhang, C. Zhang, D. Yang, L. Weng, B. Zhao, L. Wang, "Efficient click chemistry towards fatty acids containing 1,2,3-triazole: Design and synthesis as potential antifungal drugs for Candida albicans", Eur. J. Med. Chem., 136(2017), 596--602, https://doi.org/10.1016/j.ejmech.2017.05.001.

الملخص

تم تخليق مشتقين جديدين من مركبات الآزو الحلقية غير المتجانسة بتفاعل غير محفز. تم تأكيد تركيب المركبات المحضرة من خلال تقنيات مختلفة مثل 1H-NMR و 13C-NMR ومطيافية الكتلة. تمت دراسة المشتقات المحضرة وتقييمها كمثبطات للتآكل الحديد الكربوني في محلول 0.1 مولار من حمض الهيدروكلوريك. أظهرت المشتقات المحضرة

1,1'-(((1E,1'E)-(5-nitro-1,3-phenylene)bis(diazene-2,1-diyl))bis(4-methyl-3,1-phenylene))bis(1H-pyrrole-2,5-dione) (NAH)

و

1,1'-(((1E,1'E)-(5-nitro-1,3-phenylene)bis(diazene-2,1-diyl))bis(3-hydroxy-4,1-   phenylene))bis(1H-pyrrole-2,5-dione) (NAM)

كفاءة تثبيط 89.22٪ و 91.30٪ بتركيز 1 × 10-3 مولار على التوالي. وقد وجد أن الامتزاز لهذه المشتقات يتوافق مع نموذج لانغماير. بالإضافة إلى ذلك ، استخدمت نظرية الكثافة الوظيفية ومعاملات كم كيميائية اخرى لتقدير الاوربيتالات HOMO وLUMO نظريا . تشير النتائج إلى أن المشتقات المحضرة تظهر خصائص مثبطة للتآكل ، وان المشتق NAMأكثر فعالية من المشتق NAH . بالإضافة إلى ذلك ، فأن النتائج النظرية كانت متوافقة مع البيانات العملية.